
ACTIVITY RECOGNITION FOR AUTISM DIAGNOSIS

A PREPRINT

Anish Lakshapragada
Stanford University
Stanford, CA 94305
anish.lakshapragada@gmail.com

Peter Washington
Stanford University
Stanford, CA 94305
peter100@stanford.edu

Dennis Wall
Stanford University
Stanford, CA 94305
dpwall@stanford.edu

August 26, 2021

ABSTRACT

A formal autism diagnosis can be an inefficient and lengthy process. Families may wait months or longer before receiving a diagnosis for their child. One approach to lessen delays is the use digital technologies to detect the presence of behaviors indicative of autism, which in aggregate may lead to remote and automated diagnostics. One of the strongest indicators of autism is stimming, which includes repetitive, self-stimulatory behaviors such as hand flapping, headbanging, and spinning. Using computer vision to detect hand flapping is especially difficult due to the sparsity of public training data in this space and excessive shakiness and motion in such data. Our work demonstrates a novel method that may overcome these issues: we use hand landmark detection over time as a feature representation which is then fed into a Long Short-Term Memory (LSTM) model. We achieve a validation accuracy and F1 Score of about 72% on detecting whether videos from the Self-Stimulatory Behaviour Dataset (SSBD) contain hand flapping or not. Our best model also predicts accurately on external videos we recorded of ourselves outside of the dataset it was trained on. This model uses less than 26,000 parameters, providing promise for fast deployment into ubiquitous and wearable digital settings for a remote autism diagnosis.

1 Introduction

Autism affects almost 1 in 68 people in America [1] and is the fastest growing serious developmental disability in the United States [2, 3]. Despite the fact that autism can be diagnosed accurately by 24 months of age [4, 5], the average age of diagnosis is slightly less 4.5 years [6]. This is especially problematic because earlier intervention leads to better treatment outcomes [7].

Mobile digital diagnostics and therapeutics have the potential to help bridge this gap, providing scalable and accessible services to underserved populations. The use of digital and mobile therapies to support those with autism has been explored and validated in wearable devices [8–15] and smartphones [16–19]. These digital systems include machine learning models to automate the therapeutic process.

Mobile diagnostic efforts for autism using machine learning have been thoroughly explored in prior literature. Autism can be classified with high performance using 10 or less behavioral features [20–25]. While untrained humans can reliably distinguish these behavioral features [22, 26–33], an eventual goal is to move away from human-in-the-loop solutions towards fully automated and privacy-preserved diagnostic solutions [34, 35]. Preliminary efforts in this space have included automated detection of autism-related behaviors such as head banging [36], emotion evocation [37–40], and eye gaze [41].

A good indicator of autism used in diagnosis is repetitive, self-stimulatory behaviors, also known as stimming, like hand flapping, headbanging, and spinning [42]. Using deep learning for detection of hand flapping is specifically difficult due to the lack of publicly available labeled computer vision datasets of children with developmental delays. The videos which do exist are often recorded on a handheld camera which may be shaky or unstable. Here, we demonstrate a method to classify hand flapping with a novel landmark detection approach which is robust against unstable camera movement.

Here, we explore the feasibility of detecting hand flapping in unstructured home videos. We perform hand landmark detection to identify the positions of a fixed amount of hand landmarks in the image. The coordinates of the landmarks are concatenated into a single vector which is then fed into a Long-Short Term Memory (LSTM) model [43] (for each frame). We call this vector the “location frame” because it provides the locations of the hands in a single frame. We achieve 71.9% validation accuracy and an F1-score of 71.9% (70.8% precision and 74.5% recall) using 5-fold cross validation. This approach uses a low dimensional feature space, making it suitable for deployment in mobile apps.

2 Related Work

Here, we describe deep learning approaches for detection of autism-related behaviors including using gaze patterns, facial expressions, on-body device sensors, and pose estimation. Although the performances reported in each paper cannot be directly compared due to a lack of standardization of datasets, they demonstrate the feasibility of using automated computer vision methods to detect autism and related behaviors.

2.1 Gaze Patterns

Gaze patterns often differ between autism cases and controls. Chang et al. found that people with autism spend more time looking at a distracting toy than a person engaging in social behavior in a movie when compared to those with typical development [44]. This demonstrated that gaze patterns and a preference to social stimuli is an indicator of autism. Gaze patterns have been used as a feature in machine learning classifiers. Jiang et al. created a random forest classifier that used as input a subject’s performance in classifying emotions as well as other features about their gaze and face [45]. They achieved 86% accuracy for classifying autism with this approach. Liaquat et. al used convolutional neural networks (CNNs) [46] and LSTMs on a dataset of gaze patterns and achieved 60% accuracy on classifying whether somebody has autism or not [47].

2.2 Facial Expression

Another approach for autism detection is facial expression. Children with autism often evoke emotions differently than neurotypical peers. Volker et al. found that typically developing raters had more difficulty with recognizing sadness in the facial expressions of those with autism than controls [48]. This finding was confirmed by Manfredonia et. al, who used an automated facial recognition software to compare how easily those with autism and those who are NT could express an emotion when asked [49]. They found that those with autism had a harder time producing the correct facial expression when prompted compared to controls. People with autism typically have less facial symmetry [50]. Li et al. achieved an F1 score of 76% by using a CNN to extract features of facial expressions in images which were then utilized to classify autism [51]. CNNs, along with Recurrent Neural Networks (RNNs) [52], were also applied in Zunino et al.’s work where videos were used to classify autism [53]. They achieved 72% accuracy on classifying those with autism and 77% accuracy on classifying typically developing controls.

2.3 On-Body Devices

Smartwatch-based systems and sensors have been used to detect repetitive behaviors to aid intervention for those with autism. Westeyn et al. used a Hidden Markov Model to detect stimming using accelerometer data of 7 different types of self-stimulatory behaviors [54]. They reached 69% accuracy with this approach. Albinali et al. tried using accelerometers on the wrists and torsos to detect stimming in people with autism [55]. They achieved an accuracy of 88.6%. Sarker et al. used a commercially available smartwatch to collect data of adults performing stimming behaviors like headbanging, hand flapping, and repetitive dropping [56]. They used 70 features from accelerometer and gyroscope data streams to build a gradient boosting model with an accuracy of 92.6% and an F1 score of 88.1%.

2.4 Pose Estimation

Pose estimation and activity recognition have also been utilized to detect self-stimulatory behaviors. Vyas et al. retrained a 2D Mask R-CNN [57] to get the coordinates of 15 keypoints that were then transformed into a Pose Motion (PoTion) representation [58] and finally fed to a CNN model for a prediction of autism-related behavior [59]. This approach resulted in a 72.4% classification accuracy with 72% precision and 92% recall. We note that they used a derived 8349 episodes from private videos of the Behavior Imaging company to train their model. Rajagopalan et al. used the Histogram of Dominant Motions (HDM) from a video, which gives the dominant motions detected, to train a discriminatory model to detect self-stimulatory behaviors [60]. On the Self-Stimulatory Behavior Dataset (SSBD) [61], which we also use in this work, they reached 86.6% accuracy on distinguishing headbanging vs. spinning behavior and

76.3% accuracy on distinguishing headbanging, spinning, and hand flapping behavior. We note that they did not train a classifier with a control class. Another effort sought to determine whether those with autism nod/shake their head differently than neurotypical peers. They used head rotation range and amount of rotations per minute in the yaw, pitch, and roll directions as features to machine learning classifiers to detect autism [62]. They achieved 92.11% from a Decision Tree model that used the head rotation range in the roll direction and the amount of rotations per minute in the yaw direction as features.

3 Methods

To the best of our knowledge, we are the first to use just the coordinates of (hand) landmarks as features to detect hand flapping. Because our primary goal is to use machine learning classifiers in low-resource settings such as mobile devices, we strive to make our models and feature representations as light as possible.

3.1 Dataset

We use the Self-Stimulatory Behavior Dataset (SSBD) [61]. To the best of our knowledge, it is the only publicly available dataset of self-stimulatory behaviors containing examples of headbanging, hand flapping, and spinning. SSBD includes the URLs of 75 YouTube videos, and for each video the time period(s) (e.g., second 1 to second 35) when each self-stimulatory behavior was performed. There might be more than one time section in a single video for the same behavior (e.g., seconds 1 to 3 and 5 to 9 both have hand flapping), or there could be different behaviors performed in the same video at different sections (e.g., seconds 1 to 3 show headbanging and seconds 5 to 9 show hand flapping.)

3.2 Data Preprocessing

To obtain control videos (with no hand flapping), we first downloaded all of the YouTube videos from SSBD that contained sections of hand flapping. Then, the sections of hand flapping were cut out to create a new video. Parts of the video without hand flapping (i.e., the lack of being in an annotated section) were cut out to make control video clips. This data curation process is illustrated in Figure 1.

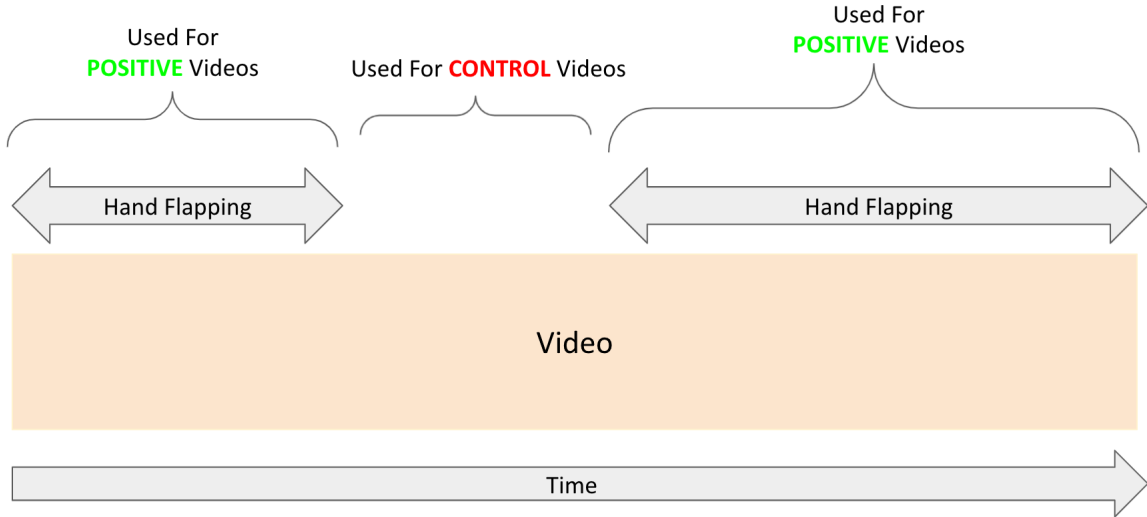


Figure 1: Process to create positive and control videos. Sections of a video that have hand flapping are cut out to make positive videos, and segments between such hand flapping sections are cut out to make control videos.

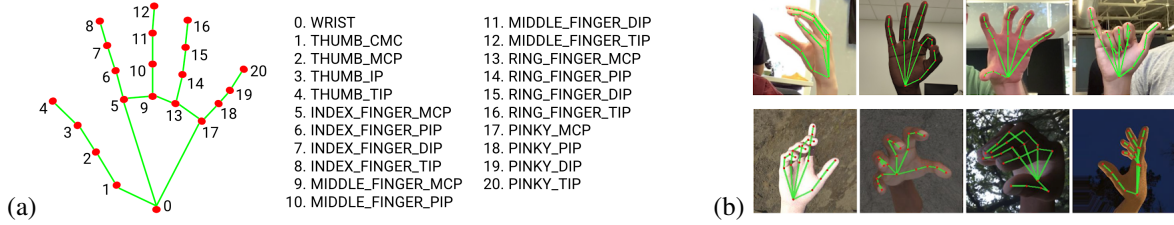


Figure 2: (a) MediaPipe’s detected hand landmarks. (b) MediaPipe’s detected hand landmarks drawn on several hands.

After extracting all positive and control clips from the downloaded videos, we aimed to maximize the amount of training data in each class. Because it only takes a few seconds to identify hand flapping, we split the video into more videos if the duration was greater than 2 seconds. We also manually deleted any videos that were shaky or low quality. Most of the videos in SSBD are of children, so to test whether a model can generalize beyond hand shape and age, we recorded 3 control videos and 3 positive videos to test our model’s robustness. ¹

3.3 Feature Extraction

When designing a model for use on a mobile device with reduced computing and battery resources, it is crucial that the number of model parameters is low enough to run efficiently. With that in mind, we try to engineer a feature representation that will not only be light but also not require heavily parameterized models like deep neural networks. We use the numerical coordinates of the detected hand landmarks as the primary feature representations.

To extract the hand coordinates, we use MediaPipe, a framework by Google that can be used to detect the landmarks on a person’s face, hands, and body [63]. MediaPipe’s hand landmark detection model provides the (x, y, z) coordinates of each of the 21 landmarks it detects on a hand. The x coordinate and y coordinate describe how far the landmark is on the horizontal and vertical dimensions, respectively. The z coordinate provide an estimation of how far the landmark is from the camera. The x , y , and z coordinates are on a scale of 0 to 1. In the case that MediaPipe does not detect a landmark, the (x, y, z) coordinates are all set to 0 for that landmark. Figure 2(a) shows the 21 hand landmarks that MediaPipe detects (as described in the MediaPipe documentation), and Figure 2(b) shows MediaPipe’s detected hand landmarks on several hands. Note that the red points in the figures are the landmarks; the green lines are only illustrated to make the hand shape more obvious.

We take the first 90 frames of a video and for each frame, concatenate the detected coordinates of a set amount of landmarks into a single vector that is then fed as input into an LSTM model. We experiment with various subsets of landmarks provided by MediaPipe; we try with all 21 landmarks, with 6 landmarks, and with ensemble methods. Note that the concatenated coordinates of landmarks will always form a vector that is 6 times larger than the number of landmarks used because there are 3 coordinates for a single landmark and 2 hands for which each landmark can be detected.

3.4 Model Architecture

The neural network architecture we use for all experiments starts with an LSTM layer with a 64-dimensional output. We take the output of the LSTM and pass it into a fully-connected layer with sigmoid activation to obtain a prediction for whether hand flapping was detected. To minimize overfitting, we also insert a dropout layer between the LSTM and the Dense layer with a dropout rate of 30%. This number of parameters of this model is shown in Table 1. Note that the number of parameters depends on the feature approach; Table 1 shows the number of parameters based on our heaviest feature approach of using all 21 landmarks.

Layer	Num. Parameters
LSTM, 64 units	48,896
Dropout, 30%	0
Dense	65
Total	48,961

Table 1: Number of parameters in the neural network.

¹Our dataset (excluding our self-recorded videos) is uploaded to Google Drive [here](#).

We experimented with other model architectures before selecting the presented model. We found that adding more than one LSTM or fully connected layer did not make any notable difference in performance; thus we removed these layers to minimize the model’s capacity for overfitting. We also experimented with the output dimensionality of the LSTM: we tried 8, 16, 32, and 64. We found that using 32 and 64 performed similarly, with 64 usually performing slightly better.

We also implemented data augmentations to minimize the chance of any overfitting that may happen due to the minimal training data. Applying these augmentations to each frame of each video was prohibitively expensive, so we decided to apply these augmentations on the low dimensional geometric location frames. We applied the same augmentation parameters for all the location frames of the same video because augmenting each location frame individually would create noise that would make it harder for the model to learn. To augment over the width dimension, we increase or decrease (with equal probability) the x coordinates such that no x coordinates would be less than 0 or greater than 1. x coordinates that were 0 before augmentation, meaning that they were not detected by MediaPipe, were set to 0 after augmentation. The same method is used for augmenting on the height and depth dimension with the y and z coordinates respectively. We try all of our feature approaches with and without augmentations. We show our overall approach in Figure 3.²

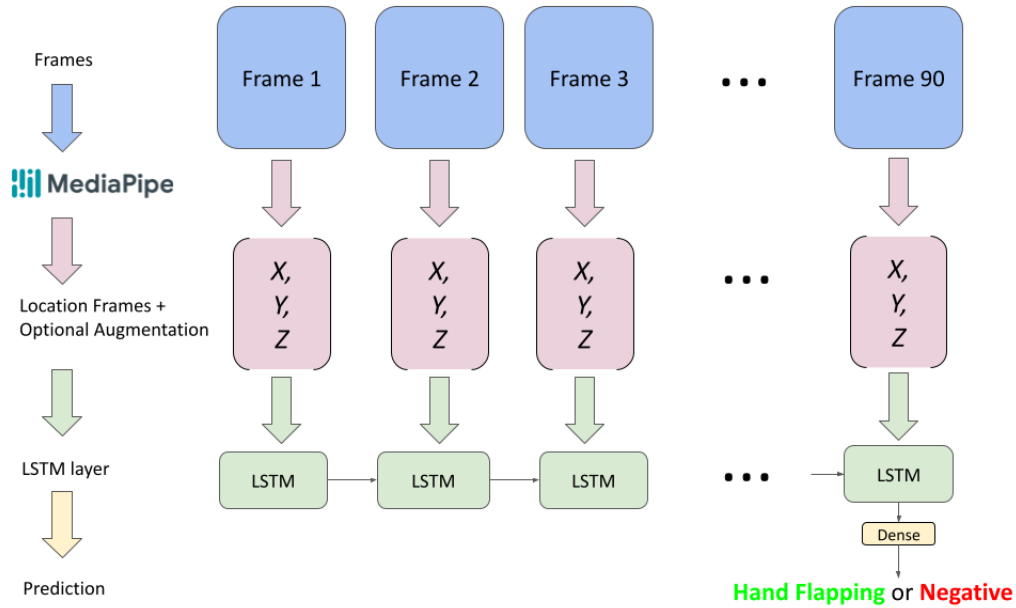


Figure 3: Our overall approach to create a prediction on whether hand flapping was detected in a video. The initial 90 frames of a single video are each converted to location frames by MediaPipe and then passed into an LSTM layer. The LSTM’s output on the last timestep goes into a Dense layer to provide a final prediction.

3.5 Feature Representations

The first feature representation approach we tried used all 21 landmarks on each hand provided by MediaPipe to create the location vector that would be fed into the LSTM. SSBD’s videos mostly contain children, whose detected hand landmarks closer together due to smaller hands. This could be a problem when generalizing the classifier for older individuals with wider gaps between hand landmarks. To help the model generalize beyond hand shape, one possible solution is to use a subset of landmarks. We use the six landmarks numbered 0, 4, 8, 12, 16, and 20 as shown in Figure 2a.

To eliminate hand shape all together, one could simply use only one landmark. We tried this method by using a single landmark at the base of the hand (numbered 0). However, because the videos in SSBD may be shaky, relying on MediaPipe’s detection of this landmark may result in empty features. One way to circumvent this problem is to take the mean of all the (x, y, z) coordinates of detected landmarks and use the average coordinate for each hand. We call this method the “mean landmark” approach.

²For conciseness in the figure, we do not show the Dropout layer between the LSTM layer and Dense layer.

3.6 Model Training

We train all of our models with binary cross-entropy loss with Adam optimization [64]. We tried learning rates of 0.0005 and 0.01. All of our models and augmentations are written using Keras [65] with a TensorFlow [66] backend. No GPUs or specialized hardware were ever required, and training a single model usually took a few minutes.

We also noticed that accuracy sometimes fluctuated up and down a bit epoch after epoch, probably due to the small dataset. We mitigate this problem by using Early Stopping to stop training if a model has not made any improvement over the last 10 epochs. After training, we revert the model’s weights to its weights on which it performed best. We used this strategy for all feature approaches.

4 Results

4.1 Evaluation Methods

We used 5-fold cross validation to evaluate each model’s average accuracy, precision, recall, and F1 score across all folds. For all approaches, we run a model ten times and record the mean and standard deviation for each of the runs’ accuracy, precision, recall, and F1 scores. We also show the mean and standard deviation of a given model’s Area under ROC Curve (AUROC) across all runs and its Receiver Operating Characteristics (ROC) curve. We compare the results of using a model with and without augmentation.

4.2 All Landmarks Approach

This approach used all of the 21 landmarks on both hands. We set the learning rate for all models with this approach to 0.0005 and train our models for 75 epochs. We show the results of this approach, with and without augmentation, in Table 2. In Figure 4, we show the ROC curves of the model with and without augmentations.

Model	Classification Accuracy	Precision	Recall	F1 Score	AUROC
Augmentation	71.2 ± 2.14	69.02 ± 2.04	79.6 ± 1.29	73.22 ± 1.28	0.76 ± 0.02
No Augmentation	72.4 ± 0.8	69.68 ± 0.99	82.92 ± 0.94	75.15 ± 0.57	0.75 ± 0.02

Table 2: Model performance when using all hand landmarks in the feature representation, with and without data augmentation.

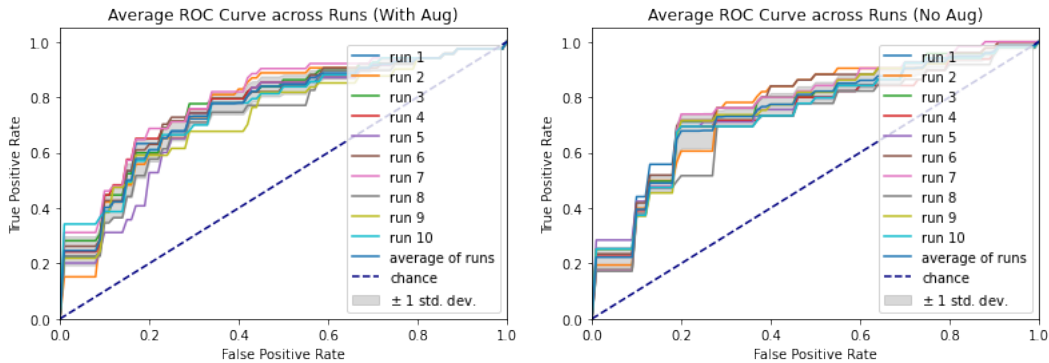


Figure 4: ROC curve of all runs and the average run for both models using all landmarks.

The model without augmentation performed better than the model with augmentation by a consistent margin of 0.5-3% on all metrics except AUROC, where it did better with a margin of 0.01. We also note that the model without augmentations achieved more consistent results (less deviation between runs), but this could be due to the stochastic nature of augmentations.

When we applied these models to the 6 hand flapping and control self-recorded videos, the model consistently made random predictions with high confidences. We hypothesize that this happened because SSBBD mainly contains children, whose hands would be smaller and detected hand landmarks closer together in contrast to the larger hands recorded in our videos.

With the all landmarks approach, we also tried using interpolation to fill in the coordinates of missing landmarks too help reduce the effects of camera instability. However, we found that using interpolation resulted in a degraded accuracy and F1 Score of 69.6% and 72.26% respectively, including higher standard deviations. Because of these results, we decided not to continue using interpolation for other approaches.

4.3 Single Landmark Approaches

In this section, we go over the mean and one landmark approaches, both of which only relied on a single landmark on each hand as the feature representation. We note that for all single landmark approaches, we used the same model as shown in Table 1 except with an LSTM with 32, and not 64, units. We find this change helps increase performance, supposedly due to it being more amenable to the smaller feature space with this approach. We also increase our learning rate to 0.01. We show the results of both approaches, with and without augmentations, in Table 3. We also show the best model’s ROC Curve in Figure 3.

Approach	Augmentation	Classification Accuracy	Precision	Recall	F1 Score	AUROC
Mean Landmark	Yes	68.1 \pm 3.69	68.04 \pm 4.19	72.72 \pm 4.92	68.27 \pm 3.34	0.72 \pm 0.02
Mean Landmark	No	69.8 \pm 4.04	69.18 \pm 5.05	69.78 \pm 6.56	67.86 \pm 3.52	0.75 \pm 0.02
One Landmark	Yes	72.8 \pm 1.16	75.29 \pm 1.72	73.1 \pm 5.09	72.6 \pm 2.30	0.77 \pm 0.02
One Landmark	No	73.9 \pm 2.77	75.84 \pm 3.68	74.96 \pm 3.88	73.92 \pm 2.56	0.78 \pm 0.03

Table 3: Model performance for mean vs. single landmark feature representations with and without data augmentation.

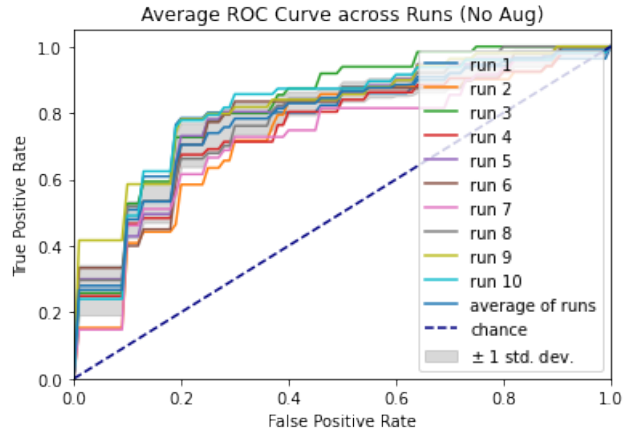


Figure 5: ROC Curve of the best model, that uses no augmentations and only takes in one landmark.

Contrary to the results of using all 21 landmarks, using augmentations in the single-landmark strategies almost always reduces the standard deviation in results. The single landmark approach consistently beat the mean landmark approach on all metrics and typically had lower standard deviations. This approach also achieved higher classification accuracy and AUROC than the all landmarks approach (without augmentation), but does not do better on recall and F1 Score.

Single landmark strategies performed better on our self-recorded videos. The all-landmarks model fails on these videos and typically gives seemingly random predictions. Using the mean landmark approach typically resulted in predictions that are “calibrated” - the lowest prediction on positive videos is higher than any predictions for control videos. However, this did not guarantee that the predictions would be accurate, as they all may be greater or smaller than 0.5 (the decision threshold.)

Using the one landmarks approach seemed to significantly reduce this issue. The predictions remained calibrated and it was less common to see all predictions greater or smaller than 0.5. Most predictions with this approach were correct. We note that on all approaches we have discussed so far, the usage of augmentations has not changed performance on our videos.

4.4 Six Landmarks Approach

In the six landmarks approach, we use the six landmarks on the edges of the hands to create the location frames. We use the same model used for the all landmarks approach (as shown in Table 1) with a learning rate of 0.01. We achieve an F1 Score and Classification Accuracy of about 72% with this approach (Table 4). We also achieve a AUROC of about 0.77 (Table 4, Figure 5).

Model	Classification Accuracy	Precision	Recall	F1 Score	AUROC
Augmentation	72.3 \pm 2.09	74.24 \pm 2.68	69.38 \pm 1.79	70.56 \pm 1.96	0.76 \pm 0.017
No Augmentation	71.9 \pm 1.7	70.78 \pm 1.85	74.5 \pm 4.04	71.9 \pm 2.25	0.765 \pm 0.027

Table 4: Model performance for feature representations containing six landmarks, with and without data augmentation.

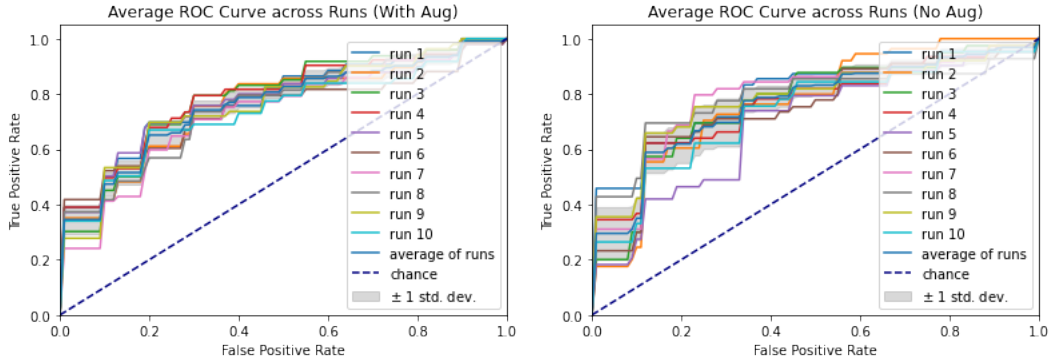


Figure 6: Graphs show the ROC curve of all runs and the average run for both models using the six landmarks approach.

The biggest change we observed with the six-landmarks approach was the quality of predictions on our videos. Predictions on our videos are almost always correct and usually have a much bigger margin between the two classes. Out of all prior approaches, we find the best success on our external videos by using the six landmarks approach. We did notice, though, that using augmentations resulted in slightly lower margins and accuracy.

5 Discussion

We used a novel feature representation to create a lightweight classifier that could achieve a high accuracy on our SSBD-derived dataset and generalize well to external videos. This approach contained only 25,921 parameters, which is of significant contrast to popular deep neural network architectures, including mobile-optimized architectures like MobileNet [67], which contain millions of parameters. Our work demonstrates that through careful feature engineering, models for autism diagnosis can be considered for use in digital therapeutics.

Using all hand landmarks resulted in the highest classification accuracy and F1 score of 72.40% and 75% respectively but worse performance on our self-recorded videos. To improve performance on our videos, we tried using single-landmark approaches of taking the mean of all detected landmarks or just tracking one landmark. We found that using one landmark approach yielded superior performance on our videos and also performed well on our internal dataset with an accuracy and F1 score both around 74%. However, using a specific set of 6 hand landmarks gave the best results on our videos. With this approach we achieved an accuracy and F1 score around 72% and very accurate results on our videos.

Interestingly, the mean landmark approach performed worse (significantly? should state) than the one landmark approach. We believe that using the mean landmark approach would be a good solution to the shakiness of the videos that may cause the one landmark to not consistently be detected. We hypothesize that the shakiness of the videos made the mean landmark approach less effective. In unstable videos, it is common for the set of landmarks detected to constantly change, so the mean of these landmarks in each frame will also always be changing. This likely added noise to the data, making performance worse.

This model does have some limitations. If model detects hand flapping when stereotypical hand motions are present even if the subject does not have autism, it will be a less reliable indicator for diagnosis. One way to work around this

problem is to use this model only in situations where it is assumed that the subject’s hand is still, such as in a salute pose. Further research would also be required to see if this model can detect hand flapping beyond the typical up-down or left-right pattern.

Beyond that, opportunities for future work include alternative feature representation and more modern model architectures such as attention-based models. Further validation is required on datasets beyond SSBD. Existing mobile therapies which collect structured videos of children with autism [16–18, 37, 40] can be used to acquire datasets to train more advanced models, and these updated models can be integrated back into the digital therapy to provide real-time feedback and adaptive experiences.

6 Acknowledgements

This work was supported in part by funds to DPW from the National Institutes of Health (1R01EB025025-01, 1R21HD091500-01, 1R01LM013083, 1R01LM013364), the National Science Foundation (Award 2014232), The Hartwell Foundation, Bill and Melinda Gates Foundation, Coulter Foundation, Lucile Packard Foundation, the Weston Havens Foundation, and program grants from Stanford’s Human Centered Artificial Intelligence Program, Stanford’s Precision Health and Integrated Diagnostics Center (PHIND), Stanford’s Beckman Center, Stanford’s Bio-X Center, Predictives and Diagnostics Accelerator (SPADA) Spectrum, Stanford’s Spark Program in Translational Research, Stanford mediaX, and Stanford’s Wu Tsai Neurosciences Institute’s Neuroscience: Translate Program. We also acknowledge generous support from David Orr, Imma Calvo, Bobby DeKesyer and Peter Sullivan. P.W. would like to acknowledge support from Mr. Schroeder and the Stanford Interdisciplinary Graduate Fellowship (SIGF) as the Schroeder Family Goldman Sachs Graduate Fellow.

References

- [1] S. Bhat, U. R. Acharya, H. Adeli, G. M. Bairy, and A. Adeli, “Autism: cause factors, early diagnosis and therapies,” *Reviews in the Neurosciences*, vol. 25, no. 6, pp. 841–850, 2014.
- [2] K. Ardhanareeswaran and F. Volkmar, “Introduction. focus: autism spectrum disorders,” *The Yale journal of biology and medicine*, vol. 88, no. 1, pp. 3–4, 2015.
- [3] E. Gordon-Lipkin, J. Foster, and G. Peacock, “Whittling down the wait time: exploring models to minimize the delay from initial concern to diagnosis and treatment of autism spectrum disorder,” *Pediatric Clinics*, vol. 63, no. 5, pp. 851–859, 2016.
- [4] C. Lord, S. Risi, P. S. DiLavore, C. Shulman, A. Thurm, and A. Pickles, “Autism from 2 to 9 years of age,” *Archives of general psychiatry*, vol. 63, no. 6, pp. 694–701, 2006.
- [5] L.-A. R. Sacrey, J. A. Bennett, and L. Zwaigenbaum, “Early infant development and intervention for autism spectrum disorder,” *Journal of Child Neurology*, vol. 30, no. 14, pp. 1921–1929, 2015.
- [6] C. for Disease Control, Prevention, *et al.*, “Spotlight on: Delay between first concern to accessing services,” 2019.
- [7] A. Estes, J. Munson, S. J. Rogers, J. Greenson, J. Winter, and G. Dawson, “Long-term outcomes of early intervention in 6-year-old children with autism spectrum disorder,” *Journal of the American Academy of Child & Adolescent Psychiatry*, vol. 54, no. 7, pp. 580–587, 2015.
- [8] N. Haber, C. Voss, J. Daniels, P. Washington, A. Fazel, A. Kline, T. De, T. Winograd, C. Feinstein, and D. P. Wall, “A wearable social interaction aid for children with autism,” *arXiv preprint arXiv:2004.14281*, 2020.
- [9] J. Daniels, J. Schwartz, N. Haber, C. Voss, A. Kline, A. Fazel, P. Washington, T. De, C. Feinstein, T. Winograd, *et al.*, “5.13 design and efficacy of a wearable device for social affective learning in children with autism,” *Journal of the American Academy of Child & Adolescent Psychiatry*, vol. 56, no. 10, p. S257, 2017.
- [10] A. Kline, C. Voss, P. Washington, N. Haber, H. Schwartz, Q. Tariq, T. Winograd, C. Feinstein, and D. P. Wall, “Superpower glass,” *GetMobile: Mobile Computing and Communications*, vol. 23, no. 2, pp. 35–38, 2019.
- [11] C. Voss, J. Schwartz, J. Daniels, A. Kline, N. Haber, P. Washington, Q. Tariq, T. N. Robinson, M. Desai, J. M. Phillips, *et al.*, “Effect of wearable digital intervention for improving socialization in children with autism spectrum disorder: a randomized clinical trial,” *JAMA pediatrics*, vol. 173, no. 5, pp. 446–454, 2019.
- [12] P. Washington, C. Voss, N. Haber, S. Tanaka, J. Daniels, C. Feinstein, T. Winograd, and D. Wall, “A wearable social interaction aid for children with autism,” in *Proceedings of the 2016 CHI Conference Extended Abstracts on Human Factors in Computing Systems*, pp. 2348–2354, 2016.

- [13] J. Daniels, J. N. Schwartz, C. Voss, N. Haber, A. Fazel, A. Kline, P. Washington, C. Feinstein, T. Winograd, and D. P. Wall, "Exploratory study examining the at-home feasibility of a wearable tool for social-affective learning in children with autism," *NPJ digital medicine*, vol. 1, no. 1, pp. 1–10, 2018.
- [14] J. Daniels, N. Haber, C. Voss, J. Schwartz, S. Tamura, A. Fazel, A. Kline, P. Washington, J. Phillips, T. Winograd, *et al.*, "Feasibility testing of a wearable behavioral aid for social learning in children with autism," *Applied clinical informatics*, vol. 9, no. 01, pp. 129–140, 2018.
- [15] C. Voss, P. Washington, N. Haber, A. Kline, J. Daniels, A. Fazel, T. De, B. McCarthy, C. Feinstein, T. Winograd, *et al.*, "Superpower glass: delivering unobtrusive real-time social cues in wearable systems," in *Proceedings of the 2016 ACM International Joint Conference on Pervasive and Ubiquitous Computing: Adjunct*, pp. 1218–1226, 2016.
- [16] H. Kalantarian, K. Jedoui, P. Washington, and D. P. Wall, "A mobile game for automatic emotion-labeling of images," *IEEE transactions on games*, vol. 12, no. 2, pp. 213–218, 2018.
- [17] H. Kalantarian, P. Washington, J. Schwartz, J. Daniels, N. Haber, and D. P. Wall, "Guess what?," *Journal of healthcare informatics research*, vol. 3, no. 1, pp. 43–66, 2019.
- [18] H. Kalantarian, K. Jedoui, P. Washington, Q. Tariq, K. Dunlap, J. Schwartz, and D. P. Wall, "Labeling images with facial emotion and the potential for pediatric healthcare," *Artificial intelligence in medicine*, vol. 98, pp. 77–86, 2019.
- [19] H. Kalantarian, P. Washington, J. Schwartz, J. Daniels, N. Haber, and D. Wall, "A gamified mobile system for crowdsourcing video for autism research," in *2018 IEEE International Conference on Healthcare Informatics (ICHI)*, pp. 350–352, 2018.
- [20] S. Levy, M. Duda, N. Haber, and D. P. Wall, "Sparsifying machine learning models identify stable subsets of predictive features for behavioral detection of autism," *Molecular autism*, vol. 8, no. 1, pp. 1–17, 2017.
- [21] J. Kosmicki, V. Sochat, M. Duda, and D. Wall, "Searching for a minimal set of behaviors for autism detection through feature selection-based machine learning," *Translational psychiatry*, vol. 5, no. 2, pp. e514–e514, 2015.
- [22] D. P. Wall, R. Dally, R. Luyster, J.-Y. Jung, and T. F. DeLuca, "Use of artificial intelligence to shorten the behavioral diagnosis of autism," 2012.
- [23] Q. Tariq, J. Daniels, J. N. Schwartz, P. Washington, H. Kalantarian, and D. P. Wall, "Mobile detection of autism through machine learning on home video: A development and prospective validation study," *PLoS medicine*, vol. 15, no. 11, p. e1002705, 2018.
- [24] Q. Tariq, S. L. Fleming, J. N. Schwartz, K. Dunlap, C. Corbin, P. Washington, H. Kalantarian, N. Z. Khan, G. L. Darmstadt, and D. P. Wall, "Detecting developmental delay and autism through machine learning models using home videos of bangladeshi children: Development and validation study," *Journal of medical Internet research*, vol. 21, no. 4, p. e13822, 2019.
- [25] P. Washington, Q. Tariq, E. Leblanc, B. Chrisman, K. Dunlap, A. Kline, H. Kalantarian, Y. Penev, K. Paskov, C. Voss, *et al.*, "Crowdsourced feature tagging for scalable and privacy-preserved autism diagnosis," *medRxiv*, 2020.
- [26] H. Abbas, F. Garberson, E. Glover, and D. P. Wall, "Machine learning approach for early detection of autism by combining questionnaire and home video screening," *Journal of the American Medical Informatics Association*, vol. 25, no. 8, pp. 1000–1007, 2018.
- [27] M. Duda, J. Kosmicki, and D. Wall, "Testing the accuracy of an observation-based classifier for rapid detection of autism risk," *Translational psychiatry*, vol. 4, no. 8, pp. e424–e424, 2014.
- [28] M. Duda, R. Ma, N. Haber, and D. Wall, "Use of machine learning for behavioral distinction of autism and adhd," *Translational psychiatry*, vol. 6, no. 2, pp. e732–e732, 2016.
- [29] P. Washington, H. Kalantarian, Q. Tariq, J. Schwartz, K. Dunlap, B. Chrisman, M. Varma, M. Ning, A. Kline, N. Stockham, *et al.*, "Validity of online screening for autism: crowdsourcing study comparing paid and unpaid diagnostic tasks," *Journal of medical Internet research*, vol. 21, no. 5, p. e13668, 2019.
- [30] P. Washington, E. Leblanc, K. Dunlap, Y. Penev, M. Varma, J.-Y. Jung, B. Chrisman, M. W. Sun, N. Stockham, K. M. Paskov, *et al.*, "Selection of trustworthy crowd workers for telemedical diagnosis of pediatric autism spectrum disorder," in *BIOCOMPUTING 2021: Proceedings of the Pacific Symposium*, pp. 14–25, World Scientific, 2020.
- [31] P. Washington, E. Leblanc, K. Dunlap, Y. Penev, A. Kline, K. Paskov, M. W. Sun, B. Chrisman, N. Stockham, M. Varma, *et al.*, "Precision telemedicine through crowdsourced machine learning: testing variability of crowd workers for video-based autism feature recognition," *Journal of personalized medicine*, vol. 10, no. 3, p. 86, 2020.

- [32] P. Washington, Q. Tariq, E. Leblanc, B. Chrisman, K. Dunlap, A. Kline, H. Kalantarian, Y. Penev, K. Paskov, C. Voss, *et al.*, “Crowdsourced privacy-preserved feature tagging of short home videos for machine learning and detection,” *Scientific reports*, vol. 11, no. 1, pp. 1–11, 2021.
- [33] P. Washington, E. Leblanc, K. Dunlap, A. Kline, C. Mutlu, B. Chrisman, N. Stockham, K. Paskov, and D. P. Wall, “Crowd annotations can approximate clinical autism impressions from short home videos with privacy protections,” *medRxiv*, 2021.
- [34] P. Washington, S. Yeung, B. Percha, N. Tatonetti, J. Liphardt, and D. P. Wall, “Achieving trustworthy biomedical data solutions,” in *BIOCOMPUTING 2021: Proceedings of the Pacific Symposium*, pp. 1–13, World Scientific, 2020.
- [35] P. Washington, N. Park, P. Srivastava, C. Voss, A. Kline, M. Varma, Q. Tariq, H. Kalantarian, J. Schwartz, R. Patnaik, *et al.*, “Data-driven diagnostics and the potential of mobile artificial intelligence for digital therapeutic phenotyping in computational psychiatry,” *Biological Psychiatry: Cognitive Neuroscience and Neuroimaging*, vol. 5, no. 8, pp. 759–769, 2020.
- [36] P. Washington, A. Kline, O. C. Mutlu, E. Leblanc, C. Hou, N. Stockham, K. Paskov, B. Chrisman, and D. Wall, “Activity recognition with moving cameras and few training examples: Applications for detection of autism-related headbanging,” in *Extended Abstracts of the 2021 CHI Conference on Human Factors in Computing Systems*, pp. 1–7, 2021.
- [37] H. Kalantarian, K. Jedoui, K. Dunlap, J. Schwartz, P. Washington, A. Husic, Q. Tariq, M. Ning, A. Kline, and D. P. Wall, “The performance of emotion classifiers for children with parent-reported autism: quantitative feasibility study,” *JMIR mental health*, vol. 7, no. 4, p. e13174, 2020.
- [38] P. Washington, H. Kalantarian, J. Kent, A. Husic, A. Kline, E. Leblanc, C. Hou, C. Mutlu, K. Dunlap, Y. Penev, *et al.*, “Training an emotion detection classifier using frames from a mobile therapeutic game for children with developmental disorders,” *arXiv preprint arXiv:2012.08678*, 2020.
- [39] P. Washington, O. C. Mutlu, E. Leblanc, A. Kline, C. Hou, B. Chrisman, N. Stockham, K. Paskov, C. Voss, N. Haber, *et al.*, “Using crowdsourcing to train facial emotion machine learning models with ambiguous labels,” *arXiv preprint arXiv:2101.03477*, 2021.
- [40] H. Kalantarian, K. Jedoui, P. Washington, Q. Tariq, M. Ning, A. Kline, J. Schwartz, K. Dunlap, and D. P. Wall, “The limitations of real-time emotion recognition for autism research,”
- [41] M. Varma, P. Washington, B. Chrisman, A. Kline, E. Leblanc, K. Paskov, N. Stockham, J.-Y. Jung, M. W. Sun, and D. P. Wall, “Identification of social engagement indicators associated with autism spectrum disorder using a game-based mobile application,” *medRxiv*, 2021.
- [42] C. for Disease Control, Prevention, *et al.*, “Signs and symptoms of autism spectrum disorders,” 2019.
- [43] S. Hochreiter and J. Schmidhuber, “Long short-term memory,” *Neural computation*, vol. 9, no. 8, pp. 1735–1780, 1997.
- [44] Z. Chang, J. M. Di Martino, R. Aiello, J. Baker, K. Carpenter, S. Compton, N. Davis, B. Eichner, S. Espinosa, J. Flowers, L. Franz, A. Harris, J. Howard, S. Perochon, E. M. Perrin, P. R. Krishnappa Babu, M. Spanos, C. Sullivan, B. K. Walter, S. H. Kollins, G. Dawson, and G. Sapiro, “Computational methods to measure patterns of gaze in toddlers with autism spectrum disorder,” *JAMA pediatrics*, April 2021.
- [45] M. Jiang, S. M. Francis, D. Srishyla, C. Conelea, Q. Zhao, and S. Jacob, “Classifying individuals with asd through facial emotion recognition and eye-tracking,” pp. 6063–6068, 2019.
- [46] Y. LeCun, B. Boser, J. S. Denker, D. Henderson, R. E. Howard, W. Hubbard, and L. D. Jackel, “Backpropagation applied to handwritten zip code recognition,” *Neural computation*, vol. 1, no. 4, pp. 541–551, 1989.
- [47] S. Liaqat, C. Wu, P. R. Duggirala, S. ching Samson Cheung, C.-N. Chuah, S. Ozonoff, and G. Young, “Predicting asd diagnosis in children with synthetic and image-based eye gaze data,” *Signal Processing: Image Communication*, vol. 94, p. 116198, 2021.
- [48] M. A. Volker, C. Lopata, D. A. Smith, and M. L. Thomeer, “Facial encoding of children with high-functioning autism spectrum disorders,” *Focus on Autism and Other Developmental Disabilities*, vol. 24, no. 4, pp. 195–204, 2009.
- [49] J. Manfredonia, A. Bangerter, N. V. Manyakov, S. Ness, D. Lewin, A. Skalkin, M. Boice, M. S. Goodwin, G. Dawson, R. Hendren, *et al.*, “Automatic recognition of posed facial expression of emotion in individuals with autism spectrum disorder,” *Journal of autism and developmental disorders*, vol. 49, no. 1, pp. 279–293, 2019.
- [50] T. Guha, Z. Yang, A. Ramakrishna, R. B. Grossman, D. Hedley, S. Lee, and S. S. Narayanan, “On quantifying facial expression-related atypicality of children with autism spectrum disorder,” in *2015 IEEE International Conference on Acoustics, Speech and Signal Processing (ICASSP)*, pp. 803–807, 2015.

- [51] B. Li, S. Mehta, D. Aneja, C. Foster, P. Ventola, F. Shic, and L. Shapiro, “A facial affect analysis system for autism spectrum disorder,” in *2019 IEEE International Conference on Image Processing (ICIP)*, pp. 4549–4553, 2019.
- [52] D. E. Rumelhart, G. E. Hinton, and R. J. Williams, “Learning internal representations by error propagation,” tech. rep., California Univ San Diego La Jolla Inst for Cognitive Science, 1985.
- [53] A. Zunino, P. Morerio, A. Cavallo, C. Ansuini, J. Podda, F. Battaglia, E. Veneselli, C. Becchio, and V. Murino, “Video gesture analysis for autism spectrum disorder detection,” in *2018 24th International Conference on Pattern Recognition (ICPR)*, pp. 3421–3426, 2018.
- [54] T. Westeyn, K. Vadas, X. Bian, T. Starner, and G. D. Abowd, “Recognizing mimicked autistic self-stimulatory behaviors using hmms,” in *Ninth IEEE International Symposium on Wearable Computers (ISWC’05)*, pp. 164–167, IEEE, 2005.
- [55] F. Albinali, M. S. Goodwin, and S. S. Intille, “Recognizing stereotypical motor movements in the laboratory and classroom: a case study with children on the autism spectrum,” in *Proceedings of the 11th international conference on Ubiquitous computing*, pp. 71–80, 2009.
- [56] H. Sarker, A. Tam, M. Foreman, N. Fay, M. Dhuliawala, and A. Das, “Detection of stereotypical motor movements in autism using a smartwatch-based system,” in *AMIA Annual Symposium Proceedings*, vol. 2018, p. 952, American Medical Informatics Association, 2018.
- [57] R. Girdhar, G. Gkioxari, L. Torresani, M. Paluri, and D. Tran, “Detect-and-Track: Efficient Pose Estimation in Videos,” in *CVPR*, 2018.
- [58] V. Choutas, P. Weinzaepfel, J. Revaud, and C. Schmid, “Potion: Pose motion representation for action recognition,” in *2018 IEEE/CVF Conference on Computer Vision and Pattern Recognition*, pp. 7024–7033, 2018.
- [59] K. Vyas, R. Ma, B. Rezaei, S. Liu, M. Neubauer, T. Ploetz, R. Oberleitner, and S. Ostadabbas, “Recognition of atypical behavior in autism diagnosis from video using pose estimation over time,” in *2019 IEEE 29th International Workshop on Machine Learning for Signal Processing (MLSP)*, pp. 1–6, 2019.
- [60] S. S. Rajagopalan and R. Goecke, “Detecting self-stimulatory behaviours for autism diagnosis,” in *2014 IEEE International Conference on Image Processing (ICIP)*, pp. 1470–1474, 2014.
- [61] S. S. Rajagopalan, A. Dhall, and R. Goecke, “Self-stimulatory behaviours in the wild for autism diagnosis,” in *2013 IEEE International Conference on Computer Vision Workshops*, pp. 755–761, 2013.
- [62] Z. Zhao, Z. Zhu, X. Zhang, H. Tang, J. Xing, X. Hu, J. Lu, and X. Qu, “Identifying autism with head movement features by implementing machine learning algorithms,” *Journal of Autism and Developmental Disorders*, pp. 1–12, 2021.
- [63] C. Lugaresi, J. Tang, H. Nash, C. McClanahan, E. Uboweja, M. Hays, F. Zhang, C.-L. Chang, M. G. Yong, J. Lee, *et al.*, “Mediapipe: A framework for building perception pipelines,” *arXiv preprint arXiv:1906.08172*, 2019.
- [64] D. P. Kingma and J. Ba, “Adam: A method for stochastic optimization,” *arXiv preprint arXiv:1412.6980*, 2014.
- [65] F. Chollet *et al.*, “Keras,” 2015.
- [66] M. Abadi, A. Agarwal, P. Barham, E. Brevdo, Z. Chen, C. Citro, G. S. Corrado, A. Davis, J. Dean, M. Devin, S. Ghemawat, I. Goodfellow, A. Harp, G. Irving, M. Isard, Y. Jia, R. Jozefowicz, L. Kaiser, M. Kudlur, J. Levenberg, D. Mané, R. Monga, S. Moore, D. Murray, C. Olah, M. Schuster, J. Shlens, B. Steiner, I. Sutskever, K. Talwar, P. Tucker, V. Vanhoucke, V. Vasudevan, F. Viégas, O. Vinyals, P. Warden, M. Wattenberg, M. Wicke, Y. Yu, and X. Zheng, “TensorFlow: Large-scale machine learning on heterogeneous systems,” 2015. Software available from tensorflow.org.
- [67] A. G. Howard, M. Zhu, B. Chen, D. Kalenichenko, W. Wang, T. Weyand, M. Andreetto, and H. Adam, “Mobilenets: Efficient convolutional neural networks for mobile vision applications,” *arXiv preprint arXiv:1704.04861*, 2017.